MOLECULAR AND CELLULAR BIOLOGY, Apr. 2010, p. 1898–1909 Vol. 30, No. 8
0270-7306/10/$12.00 doi:10.1128/MCB.01199-09

The Chaperone-Like Protein HYPK Acts Together with NatA in Cotranslational N-Terminal Acetylation and Prevention of Huntingtin Aggregation[▽]†

Thomas Arnesen,[1,2,3]* Kristian K. Starheim,[1,2,3] Petra Van Damme,[4,5] Rune Evjenth,[1] Huyen Dinh,[1] Matthew J. Betts,[6] Anita Ryningen,[7] Joël Vandekerckhove,[4,5] Kris Gevaert,[4,5] and Dave Anderson[8]‡

Department of Molecular Biology, University of Bergen, N-5020 Bergen, Norway[1]; Department of Surgical Sciences, University of Bergen, N-5020 Bergen, Norway[2]; Department of Surgery, Haukeland University Hospital, N-5021 Bergen, Norway[3]; Department of Medical Protein Research, VIB, B-9000 Ghent, Belgium[4]; Department of Biochemistry, Ghent University, B-9000 Ghent, Belgium[5]; EMBL, Meyerhofstrasse 1, 69117 Heidelberg, Germany[6]; Department of Medicine, Haukeland University Hospital, N-5021 Bergen, Norway[7]; and Institute of Molecular Biology, University of Oregon, Eugene, Oregon 97403-1229[8]

Received 3 September 2009/Returned for modification 26 October 2009/Accepted 27 January 2010

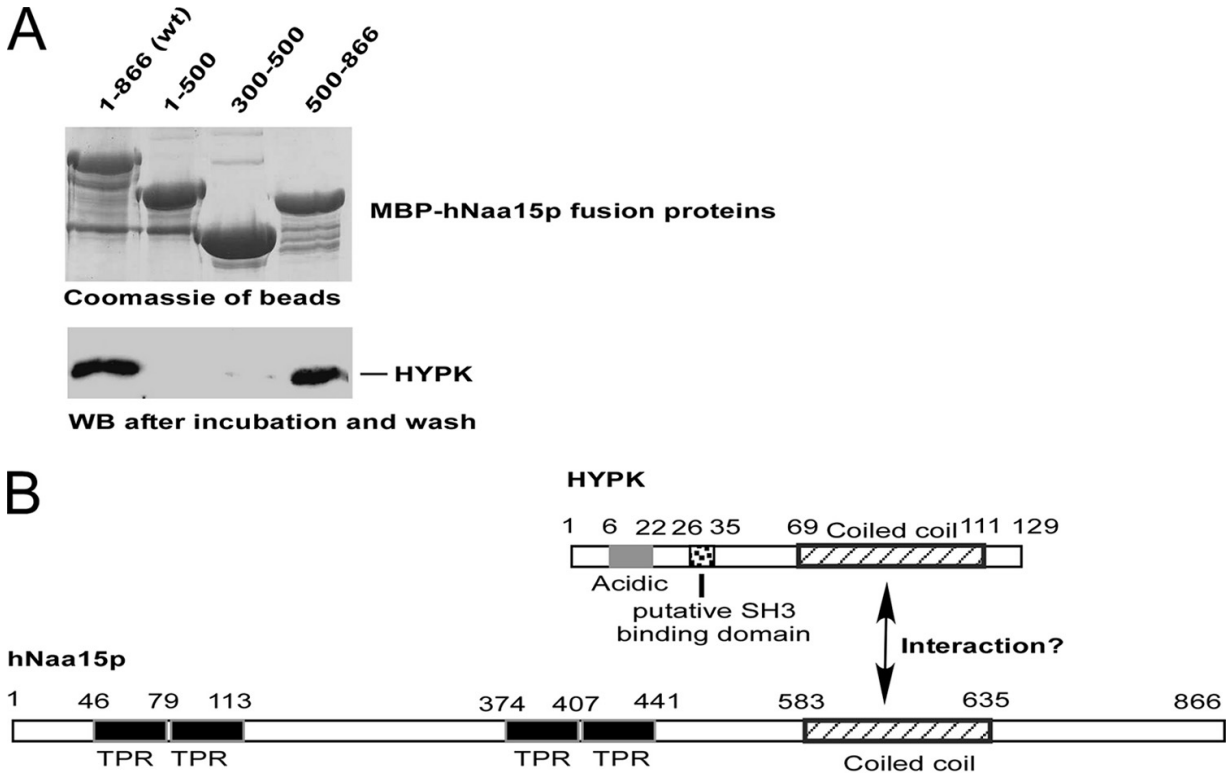

FIG. 1. The C terminus of hNaa15p interacts directly with HYPK. (A) Purified MBP-hNaa15p fusion proteins containing N-terminal MBP and a His tag fused to a segment of the hNaa15p protein, as indicated, were purified and bound to Ni-affinity beads. HYPK was separately fully purified and added to the beads containing different MBP-hNaa15p fusions. After incubation with rotation for 10 min and several washing steps, the MBP-hNaa15p beads were analyzed for HYPK binding by SDS-PAGE and Western blotting using anti-HYPK. A positive signal indicates that purified HYPK binds to the MBP-hNaa15p fusion protein. Equal amounts of the different MBP-hNaa15p fusions used were confirmed by SDS-PAGE and Coomassie staining. (B) Schematic model of the predicted domains of hNaa15p and HYPK and the potential regions involved in the hNaa15p-HYPK interaction. TPR, tetratricopeptide repeat.

A

1 MRRRGEIDMATEGDVELELETETSGPERPPEKPR **KHDSGAADLER** **VTDYAEEK**

54 **EIQSSNLETAMSVIGDRR** SREQKAKQEREKELAKVTIK **KEDLELIMTEMEISR**

107 AAAERSLR **EHMGNVVEALIALTN**

B

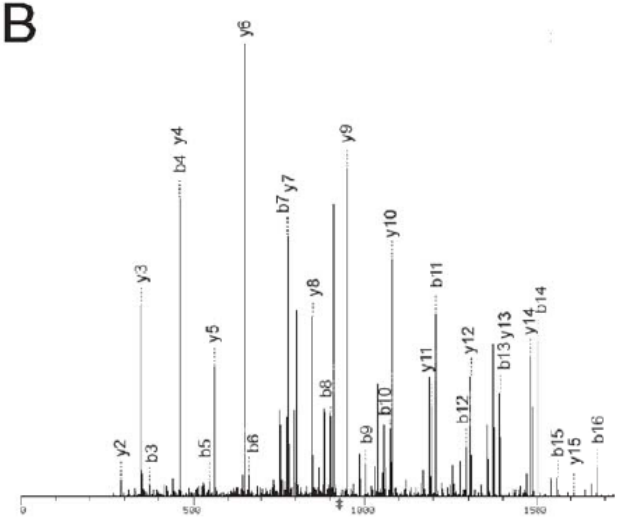

Seq	#	b	y	#
E	1	130.1	1851.0	17
I	2	243.3	1721.9	16
Q	3	371.4	1608.8	15
S	4	458.5	1480.6	14
S	5	545.6	1393.6	13
N	6	659.7	1306.5	12
L	7	**772.8**	**1192.4**	11
E	8	901.9	1079.2	10
T	9	1003.1	950.1	9
A	10	1074.1	849.0	8
M	11	1205.3	777.9	7
S	12	1292.4	646.7	6
V	13	1391.5	559.6	5
I	14	1504.7	460.5	4
G	15	1561.7	347.4	3
D	16	1676.8	290.3	2
R	17	1833.0	175.2	1

Supplementary figure S1. HYPK identified in hNaa10p-hNaa15p immunoprecipitates. (A) The amino acid sequence of the HYPK protein is shown, with the identified tryptic peptides from anti-hNaa10p and anti-hNaa15p affinity extracts in bold and underlined. Based on the HYPK-specific peptides identified by MS/MS in our immunoprecipitation experiments, we are not able to distinguish between the three potential variants of HYPK. (B) MS/MS spectrum of the HYPK peptide ^{54}EIQSSNLETAMSVIGDR^{70}, identified in a hNaa10p affinity extraction. The peptide precursor ion current was 2.16 x 10 5. The fragments of the +2 peptide precursor ion fragments were identified by the program SEQUEST (16) as +1 individual b or y ions, which are labeled in the spectrum. Almost all major peaks are assigned; the peptide had an Xcorr of 4.58, and a probability of correct sequencing, based on a machine learning analysis of the mass spectrometry data and SEQUEST parameters (Anderson, D. C. *et al*., *J.Proteome.Res*. 2003 **2**:137-146) of 99%. The mass assignments for the individual b and y ions are shown in the inset table, with the major matched ions indicated in bold.

TABLE S1. Overview of HYPK peptides identified in hNaa10p-hNaa15p immunoprecipitates[a].

HYPK peptides	anti-hNaa15p extracts peptide probability	anti-hNaa10p extracts peptide probability
^{92}KEDLELIMTEMEISR^{106}	0.99	0.98
^{54}EIQSSNLETAMSVIGDR^{70}	-	0.99
^{35}KHDSGAADLER^{45}	0.95	0.98
^{93}EDLELIMTEMEISR^{106}	0.65	0.94
^{92}KEDLELIM#TEM#EISR^{106}	0.50	0.93
^{46}VTDYAEEK^{53}	0.92	0.86
^{93}EDLELIM#TEM#EISR^{106}	0.85	-
^{115}EHM#GNVVEALIALTN^{129}	0.84	0.54
^{54}EIQSSNLETAMSVIGDRR^{71}	0.74	-
^{54}EIQSSNLETAM#SVIGDR^{70}	0.61	0.57
^{93}EDLELIMTEM#EISR^{106}	0.58	-
^{46}VTDYAEEKEIQSSNLETAM#SVIGDR^{70}	0.52	-

HYPK (gi|27734984) was identified in 4 of 4 hNaa10p and hNaa15p affinity extracts.

[a]Each peptide was sequenced multiple times in a number of different 2D lc/ms/ms runs. The probabilities of correct peptide sequencing were derived from support vector machine learning calculations (Anderson, D. C. *et al*., *J.Proteome.Res*. 2003 **2**:137-146). M# refers to oxidized methionine.

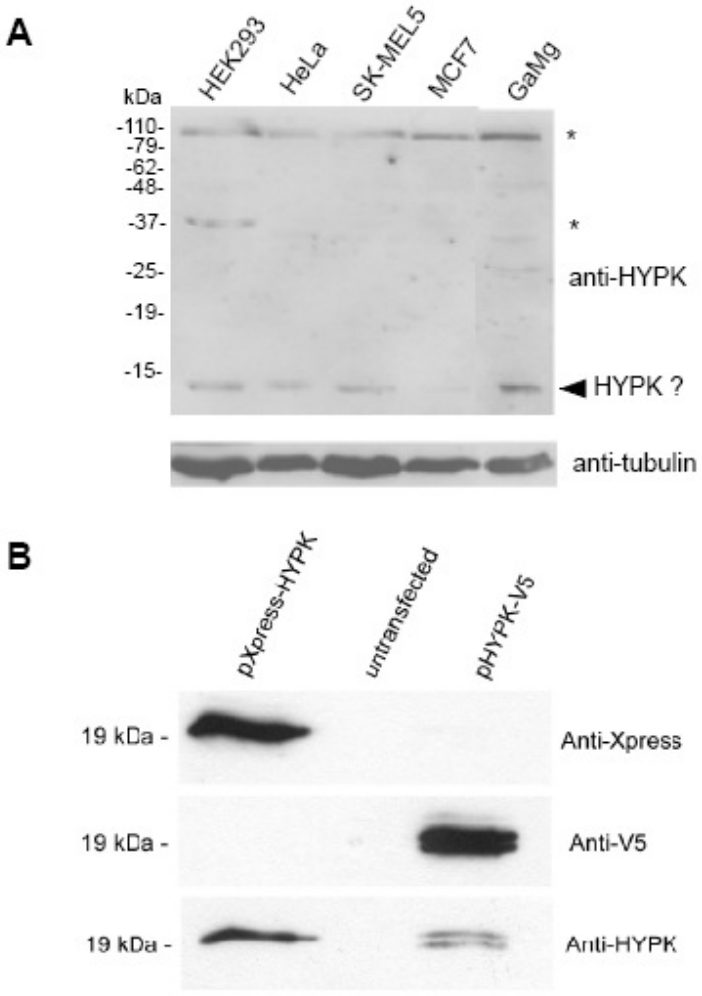

Supplementary figure S2. Test of anti-HYPK antibody. (A) Lysates of different human cell lines were applied to SDS-PAGE and Western blotting as indicated (see also materials and methods) using anti-HYPK and anti-β-tubulin. A band at ~15 kDa most likely representing HYPK is indicated. The asterisks indicate bands possibly representing unspecificity or perhaps slower migrating forms/complexes of HYPK. (B) HEK293 cells were transfected with plasmids pXpress-*HYPK*, p*HYPK*-V5 or no plasmid as indicated. After 48 hours cells were harvested and the resulting lysates processed by SDS-PAGE and Western blotting using anti-Xpress, anti-V5 and anti-HYPK.

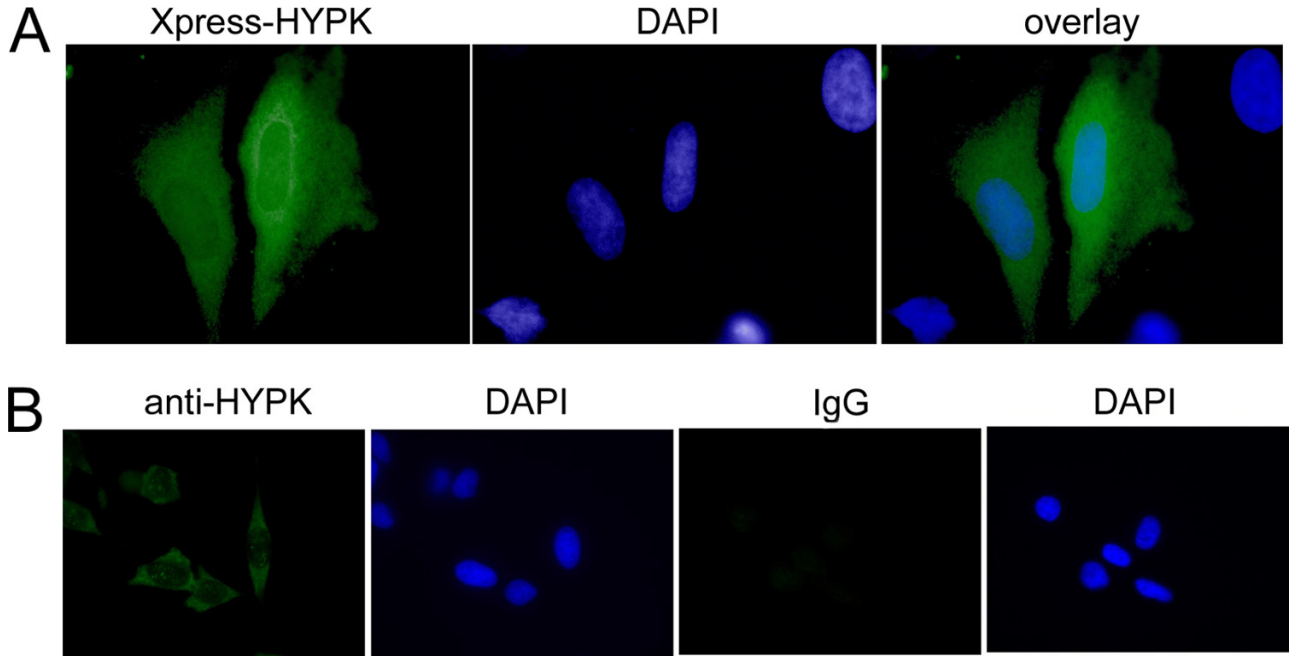

FIG. 2. Subcellular localization of HYPK. (A) (Left) HeLa cells were transfected with a plasmid encoding Xpress-HYPK, and at 48 h posttransfection, cells were fixed and anti-Xpress antibodies and Alexa 488-conjugated anti-mouse antibodies were used to visualize Xpress-HYPK. (Middle) DAPI (4′,6-diamidino-2-phenylindole) staining was used to visualize the nuclei of the cells. (Right) Overlay of DAPI and Xpress-HYPK signals. More than 200 transfected cells were inspected, and representative cells are shown. (B) Twenty-four hours after being seeded, HeLa cells were fixed and anti-HYPK and Alexa 488-conjugated anti-rabbit antibodies were used to visualize endogenous HYPK. Rabbit IgG was used as an unspecific negative control. DAPI staining is presented next to each sample to visualize nuclei and verify the presence of cells. Pictures are representative of three independent experiments in which at least 100 cells were taken into account.

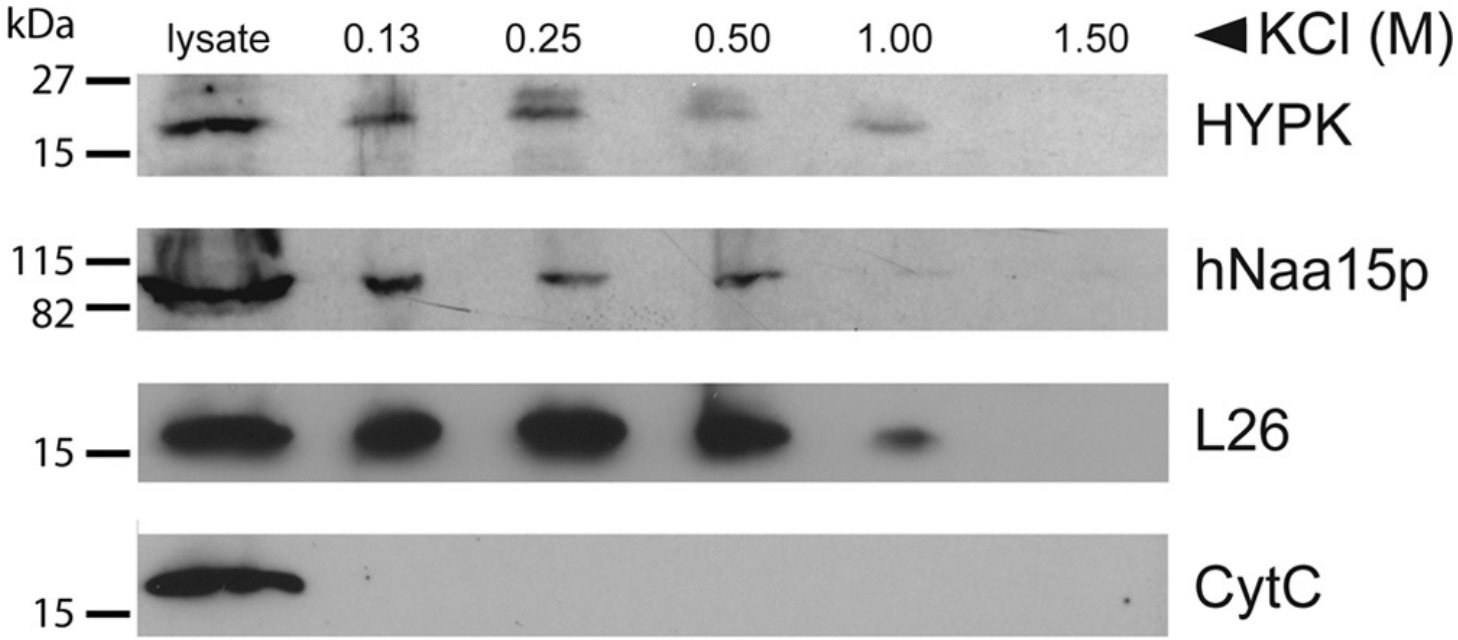

FIG. 3. HYPK cosediments with polysomal fractions in a salt-sensitive manner. Polysomal pellets from HeLa cells were resuspended in buffer containing increasing concentrations of KCl. Cell lysate and polysomal pellets after KCl treatment were analyzed by SDS-PAGE and Western blotting. The membrane was incubated with anti-HYPK, anti-hNaa15p, anti-L26 (ribosomal protein), and anti-CytC antibodies. Molecular mass markers (in kDa) are indicated on the left. Results shown are representative of three independent experiments.

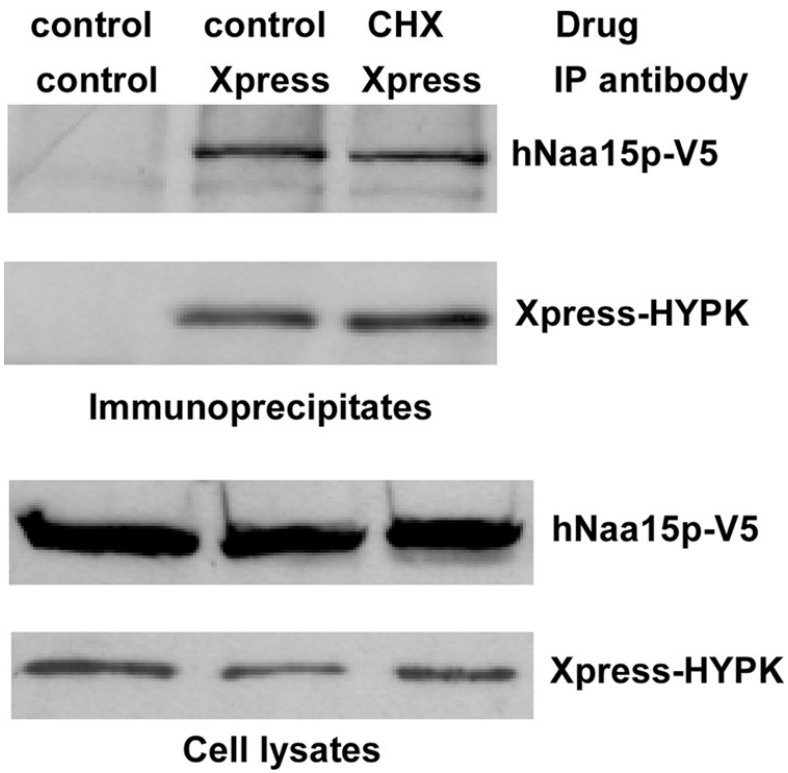

FIG. 4. HYPK-hNaa15p interaction is independent of active translation. HEK293 cells were cotransfected with plasmids expressing Xpress-HYPK and hNaa15p-V5. At 48 h posttransfection, cells were treated with 50 μg/ml cycloheximide (CHX) or solvent (control) for 30 min. The cells were then harvested and subjected to immunoprecipitation (IP), using anti-Xpress or negative-control antibodies. The presence of hNaa15-V5 in complex with Xpress-HYPK was analyzed by SDS-PAGE and Western blotting, using anti-V5. The inhibitory effect of CHX on protein translation was verified in parallel samples detecting the reduction of unstable proteins. The results shown are representative of three independent experiments.

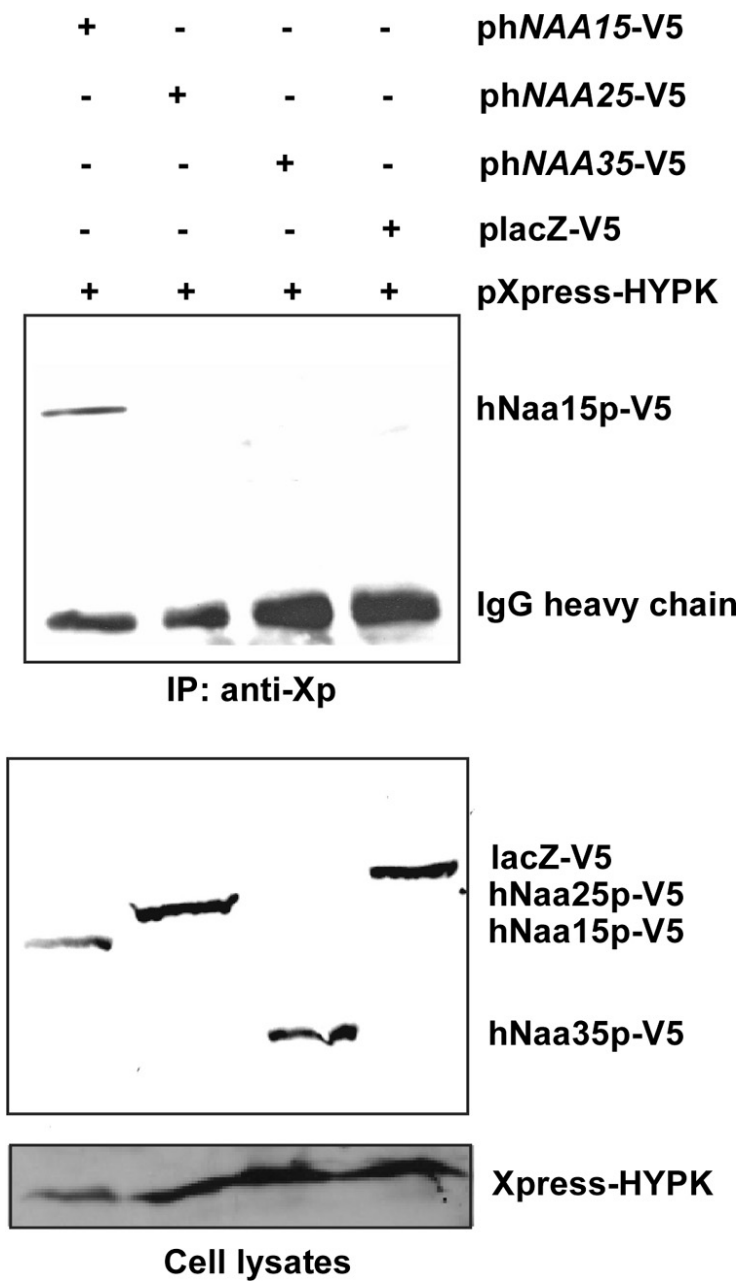

FIG. 5. HYPK interacts specifically with hNaa15p of hNatA, not with hNaa25p of hNatB and hNaa35p of hNatC. HEK293 cells were cotransfected with plasmids encoding Xpress-HYPK plus hNaa15p-V5, hNaa25p-V5, hNaa35p-V5, or lacZ-V5, as indicated. At 48 h posttransfection, cells were harvested and subjected to immunoprecipitation using anti-Xpress (anti-Xp) antibodies. The presence of hNaa15p-V5, hNaa25p-V5, and hNaa35p-V5 in complex with Xpress-HYPK was investigated by SDS-PAGE and Western blotting, using anti-V5. (Top) Western blot of immunoprecipitates. (Bottom) Western blot of cell lysates prior to immunoprecipitation. The results shown are representative of three independent experiments.

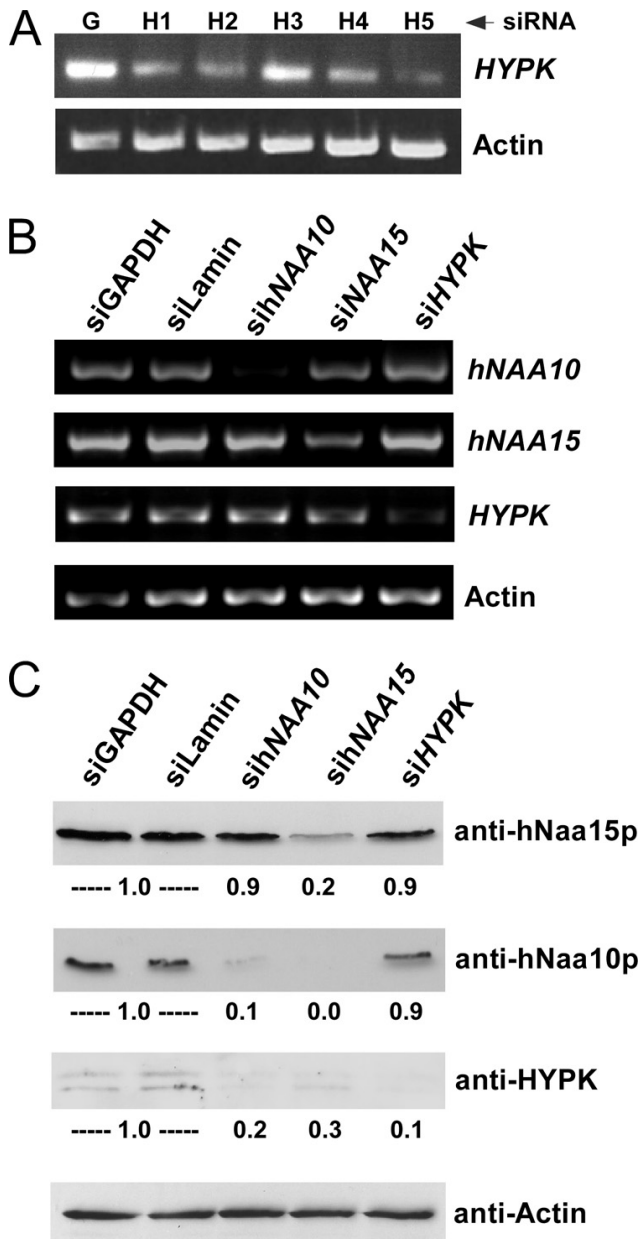

FIG. 6. siRNA-mediated knockdown of *HYPK*, h*NAA10*, and h*NAA15*. (A) Five individual siRNAs potentially targeting *HYPK* expression (H1 to H5) were tested by siRNA transfection of HeLa cells and subsequent RT-PCR analysis at 48 h posttransfection, using primers specific for *HYPK* and β-actin. G, si*GAPDH* (negative control). (B) siRNA-mediated knockdown in HeLa cells of the specific genes *HYPK*, h*NAA10*, and h*NAA15*, as indicated. siLamin and siGAPDH were used as negative controls. si*HYPK* is an equal mixture of the four effective si*HYPK* siRNAs shown in panel A (H1, H2, H4, and H5; 50 nM total concentration). RT-PCR analysis was performed at 72 h posttransfection. (C) SDS-PAGE and Western blotting, using anti-HYPK, anti-hNaa10p, anti-hNaa15p, and antiactin, of HeLa samples treated identically to those described for panel B. Protein levels were quantified using a Fuji Film IR LAS 1000 documentation system and Image Gauge 3.45. Protein levels in siLamin- and siGAPDH-treated cells (the mean for these two negative controls) were set to 1.0, and protein levels in sih*NAA10*-, sih*NAA15*-, and si*HYPK*-treated cells were estimated relative to this and normalized to actin levels. HYPK appeared as one or two specific bands, and the sum of the two was used for quantification. All results are representative of at least three independent experiments.

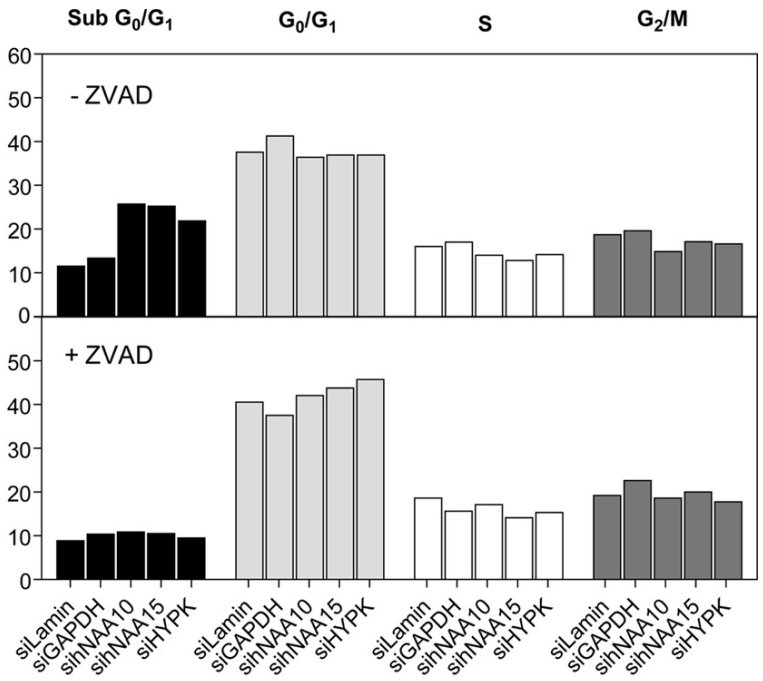

		Sub G_0/G_1	G_0/G_1	S	G_2/M
- ZVAD	siLamin	11.5	37.6	16.0	18.7
	siGAPDH	13.4	41.3	17.0	19.6
	sihNAA10	25.7	36.4	14.0	14.9
	sihNAA15	25.2	36.9	12.8	17.1
	siHYPK	21.9	36.9	14.2	16.6
+ ZVAD	siLamin	8.9	40.6	18.6	19.2
	siGAPDH	10.4	37.5	15.6	22.6
	sihNAA10	10.9	42.1	17.1	18.6
	sihNAA15	10.5	43.8	14.1	20.0
	siHYPK	9.5	45.7	15.3	17.8

FIG. 7. *HYPK* knockdown induces cell death and G_1/G_0 cell cycle arrest. Flow cytometric cell cycle analysis of *HYPK*, h*NAA10*, and h*NAA15* knockdown cells was performed at 72 h posttransfection. siLamin- and siGAPDH-treated samples were used as negative controls. (Top panels) No ZVAD treatment. (Bottom panels) ZVAD treatment to inhibit caspase activity and, thereby, induction of caspase-mediated cell death. Experiments were performed three times, and representative values are given.

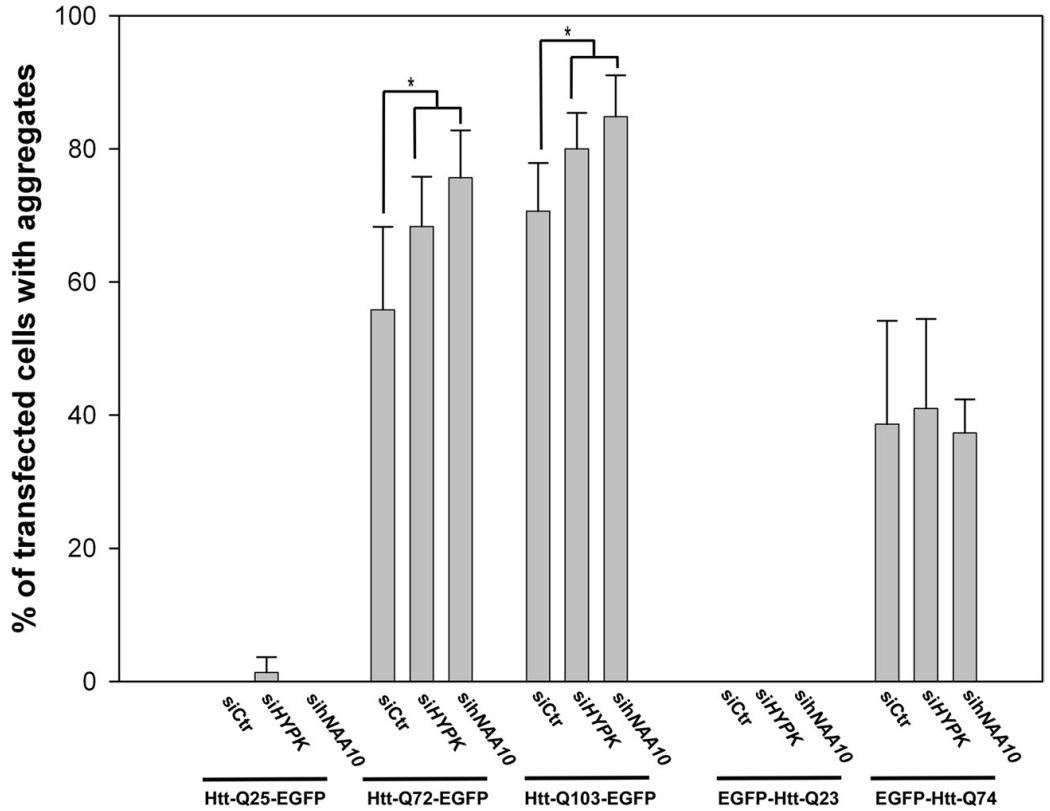

FIG. 8. *HYPK* and h*NAA10* knockdown increases Huntingtin aggregation. HeLa cells were transfected with the indicated siRNAs, and at 24 h posttransfection, the medium was replaced and the cells were transfected with plasmids encoding the indicated Htt-EGFP fusion proteins. Twenty-four hours after plasmid transfection, the cells were fixed, cells displaying Htt-EGFP aggregates were counted, and the percentage of cells with aggregates among the transfected cells was calculated. At least 200 transfected cells were counted per sample, and values presented are means ± standard deviations (SD) for three to six independent experiments. P values for independent t tests for samples versus control are indicated with asterisks ($P < 0.05$).

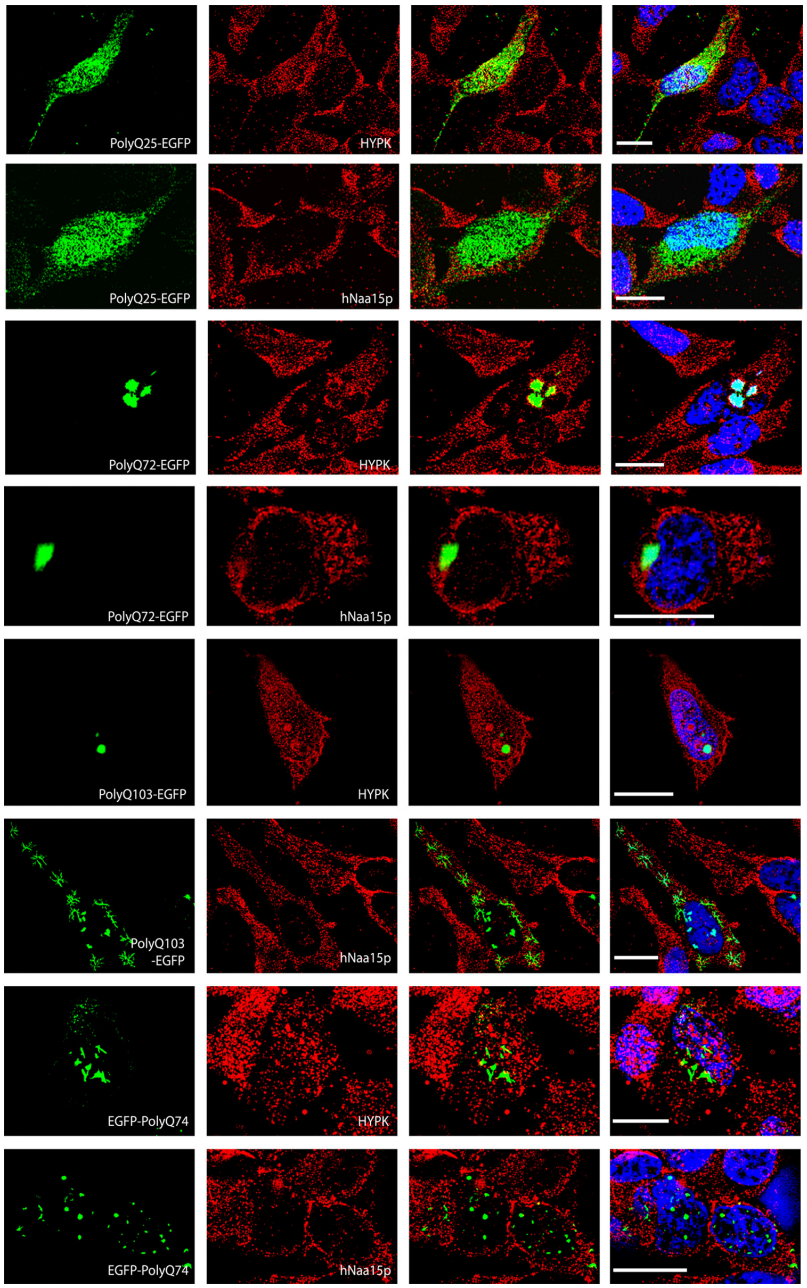

FIG. 9. HYPK and hNaa15p do not colocalize with Htt aggregates. HeLa cells expressing various EGFP-tagged polyQ versions (left column) were incubated with HYPK- or hNaa15p-specific antibodies, as indicated in the figure (second column from left). Alexa 594-conjugated anti-mouse antibodies were used to visualize HYPK and hNaa15p. The third column from left presents an overlay of polyQ-EGFP and HYPK or hNaa15p. DAPI staining was used to visualize DNA, as included in the overlay shown in the right column. Images were processed by deconvolution (Leica 4000 software). Bar, 25 μm.

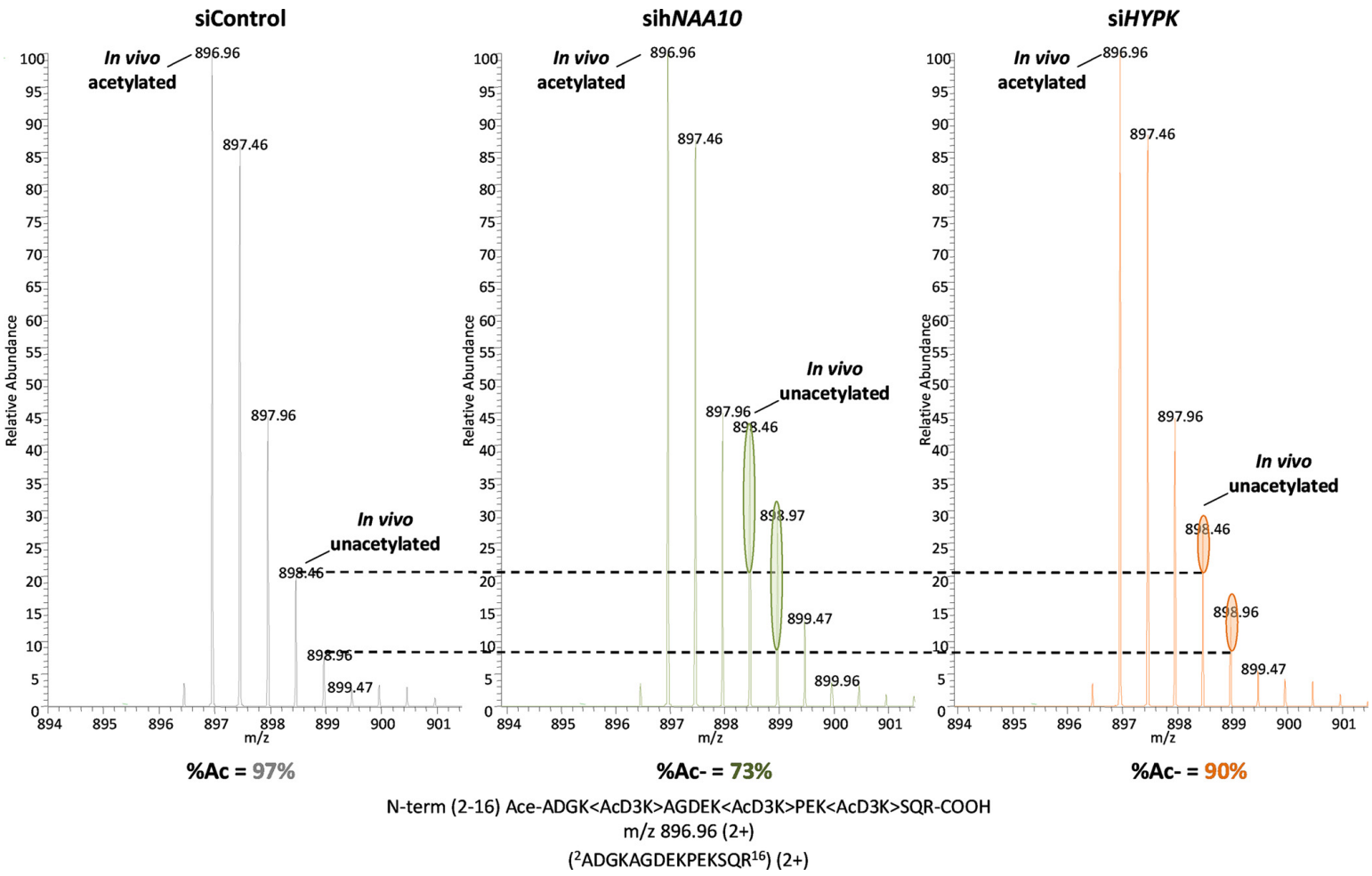

FIG. 10. *HYPK* knockdown reduces NatA-mediated N-terminal acetylation. HeLa cells were transfected with siRNAs targeting h*NAA10*, *HYPK*, or a control. At 24 h posttransfection, the medium was replaced and cells transfected with pPCNP-V5 plasmid. Forty-eight hours after plasmid transfection, the cells were harvested and lysed, and PCNP-V5 was immunoprecipitated and processed as described in Materials and Methods. ZVAD was added every 24 h to prevent induction of apoptosis. MS spectra of doubly charged peptide ions originating from the N terminus of PCNP (GenBank accession no. Q8WW12) are shown. The peptide was identified as 2-ADGKAGDEKPEKSQR-16. The extent of PCNP N^{α} acetylation, as determined by an MS isotope pattern calculator (http://prospector.ucsf.edu), was calculated as being 97%, 73%, and 90% in the control, sih*NAA10*, and si*HYPK* samples, respectively. The ellipsoids indicate the relative increases of the *in vivo* unacetylated N terminus of PCNP in the sih*NAA10*- and si*HYPK*-treated samples compared to that in the control sample. The data are representative of two independent experiments.

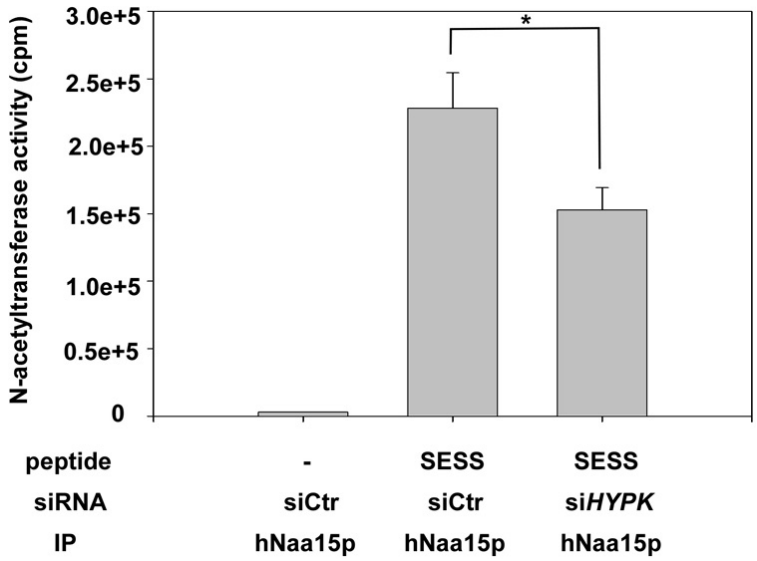

FIG. 11. hNatA immunoprecipitated from *HYPK* knockdown cells displays reduced *in vitro* acetylation activity. HeLa cells (approximately 5×10^6 per sample) were transfected with the indicated siRNAs, and at 24 h posttransfection, ZVAD was added to prevent induction of apoptosis. After 48 h, the cells were harvested and lysed, and the lysate was subjected to immunoprecipitation (IP) using an anti-hNaa15p specific antibody. The beads containing functional hNatA complexes were analyzed for N^{α}-acetyltransferase activity, using [^{14}C]acetyl-CoA and a Ser-Asp-Ser-Ser (SESS)-starting 24-mer peptide known to be acetylated by NatA *in vitro*. The amount of acetyl incorporation was determined by isolation of the peptides followed by scintillation counting. Verification of knockdown and the presence of equal levels of hNaa15p in the immunoprecipitates were routinely confirmed. Experiments were performed three times, and values are means $\pm$ SD. *P* values for independent *t* tests for si*HYPK* samples versus control are indicated with an asterisk ($P < 0.05$).

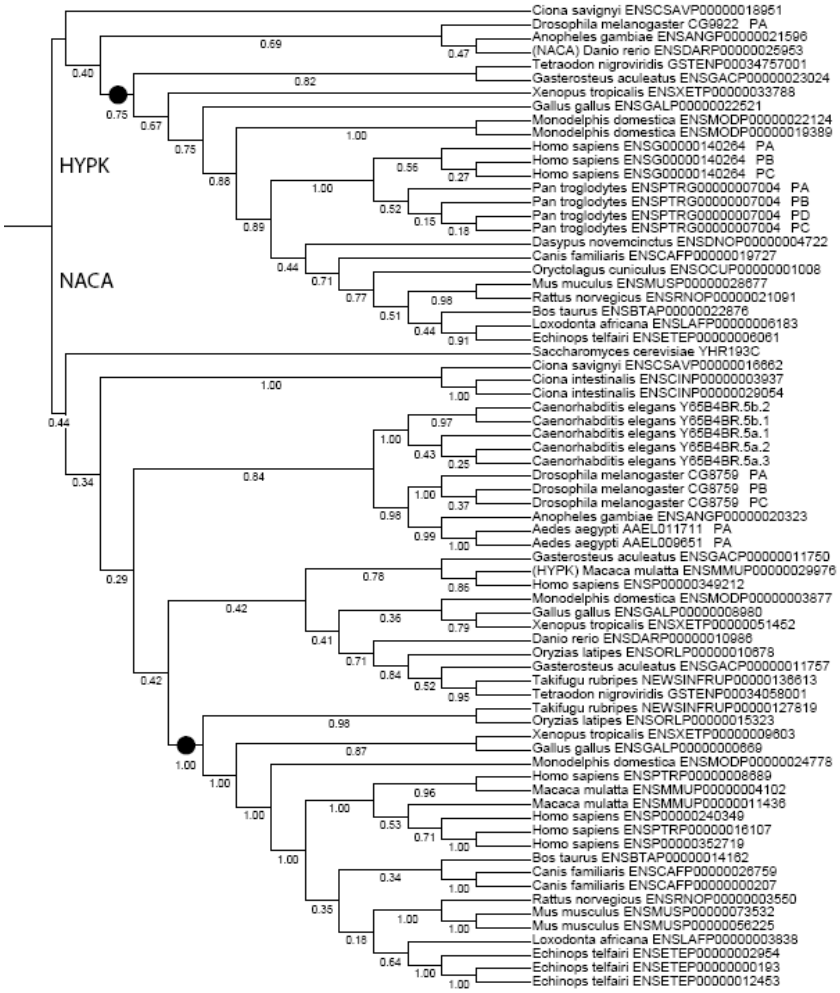

Supplementary figure S3. Evolutionary origin of HYPK. The ancestor of HYPK/NACA probably duplicated sometime after the fungi and metazoa separated, since metazoa have both HYPK and NACA, but yeast only has NACA. *C. elegans* only seem to have NACA, in contrast to fruitfly and mosquito, which have both genes. Phylognetic tree of sequences from Ensembl families (see methods), with transcripts identified by species names and Ensembl transcript identifiers and rooted in a way that maximises the separation between the families. All genes below the named branch are from the named family, except where noted. The branch support values indicate some overlap between the groups, which is natural from an automatic definition (as used by Ensembl) of families that are related. The two branches marked with a circle have support values >= 0.75 and more confidently indicate the split between HYPK and NACA. Tree drawn with iTOL (Letunic I and Borch P, *Bioinformatics*, 2007 **23**:127-8).